

Aluminocerite-Ce: A new species from Baveno, Italy: Description and crystal-structure determination

FABRIZIO NESTOLA,^{1,*} ALESSANDRO GUASTONI,¹ FERNANDO CÁMARA,² LUCIANO SECCO,¹
ALBERTO DAL NEGRO,¹ DANILO PEDRON,³ AND ANTON BERAN⁴

¹Dipartimento di Geoscienze, Università di Padova, Via Giotto 1, 35137, Padova, Italy

²C.N.R., Istituto di Geoscienze e Georisorse, Unità di Pavia, Via Ferrata 1, 27100 Pavia, Italy

³Dipartimento di Scienze Chimiche, Università di Padova, Via Marzolo 1, 35131, Padova, Italy

⁴Institute of Mineralogy and Crystallography, University of Vienna, Althanstrasse 14, 1090 Vienna, Austria

ABSTRACT

Aluminocerite-(Ce), ideally $(\text{Ce,Ca})_9\text{Al}(\text{SiO}_4)_3[\text{SiO}_3(\text{OH})]_4(\text{OH})_3$, is isostructural with cerite-(Ce) and cerite-(La). The holotype was found at the Ratti quarry, near Baveno, Italy, in millimeter-sized secondary cavities hosted in aplite-pegmatite veins and pods within pink granite. Aluminocerite-(Ce) forms aggregates of pseudo-octahedral to rhombohedral crystals flattened on the *c* axis. The cotype of aluminocerite-(Ce) was discovered at the Locately quarry, also near Baveno, where it occurs in centimeter-sized miarolitic cavities in pink granite. The mineral is pale pink to pink-reddish, with a white streak, and is translucent with a vitreous luster. Aluminocerite-(Ce) is non-fluorescent. The hardness based on the Mohs scale is 5, and the tenacity is brittle. Neither cleavage, fracture, or twinning were observed. Calculated density is 4.675 g/cm³. It is uniaxial, optically positive, with $n_o = 1.810$ – 1.816 and $n_e = 1.812$ – 1.822 ($\lambda = 589$ nm) and non-pleochroic. The average of 15 electron microprobe analyses for the holotype gave (wt%): Ce₂O₃ 23.37; Nd₂O₃ 15.59; La₂O₃ 7.43; Sm₂O₃ 4.38; Pr₂O₃ 3.54; Gd₂O₃ 3.12; Y₂O₃ 1.68; Dy₂O₃ 0.46; Yb₂O₃ 0.07; CaO 8.31; Fe₂O₃ 0.47; Al₂O₃ 2.47; SiO₂ 24.01; and H₂O 3.63 (calculated from crystal-chemical constraints), total 98.53 wt%, corresponding to the empirical formula $(\text{Ca}_{2.60}\text{Ce}_{2.49}\text{Nd}_{1.62}\text{La}_{0.80}\text{Sm}_{0.44}\text{Pr}_{0.38}\text{Gd}_{0.30}\text{Y}_{0.26}\text{Dy}_{0.04}\text{Yb}_{0.01})_{\Sigma 8.94}(\text{Al}_{0.85}\text{Fe}_{0.10})_{\Sigma 0.95}(\text{SiO}_4)_3[\text{SiO}_3(\text{OH})]_4(\text{OH})_{3.06}$, calculated on the basis of Si = 7. Aluminocerite-(Ce) is trigonal, space group *R*3*c*, with $a = 10.645(1)$, $c = 38.019(5)$ Å, $V = 3731$ Å³. The strongest eight lines in the X-ray powder diffraction pattern are [d in Å (I)(hkl)]: 3.405(27)(122), 3.250(26)(124), 2.914(100)(02,10), 2.647(58)(220), 2.198(40)(03,12), 1.923(34) (238), 1.826(24)(051), and 1.732(46)(03,18). The crystal structure has been refined to $R1 = 0.056$ for 745 observed reflections. The name is an allusion to the fact that it is the Al-dominant analog of cerite-(Ce).

Keywords: Aluminocerite-(Ce), single-crystal XRD, EMP analyses, new mineral, Raman spectroscopy

INTRODUCTION

Cerite-(Ce) is a rare-earth element (REE) silicate with formula $(\text{REE,Ca})_9(\text{Mg,Fe}^{3+})(\text{SiO}_4)_3[\text{SiO}_3(\text{OH})]_4(\text{OH})_3$. It was first described from the Bastnäs skarn deposit, Skinnsätterberg District, South-Central Sweden, by Hisinger and Berzelius (1804). A recent chemical reinvestigation of cerite-(Ce) samples from several Bastnäs type deposits from the Riddarhyttan ore field, Sweden, showed Mg > Fe³⁺ only in the octahedral *M* site, with Al being found to be below the detection limit of electron microprobe for these samples (Holtstam and Andersson 2007). The crystallography of cerite-(Ce) from Mountain Pass, California, and Bastnäs, Sweden has been investigated by several authors (Gay 1957; Glass et al. 1958), and the crystal structure of cerite-(Ce) was solved and refined by Moore and Shen (1983) using crystals from Mountain Pass. This study demonstrated that the octahedral *M* site in this material has a site occupancy

of $(\text{Mg}_{0.6}\text{Fe}_{0.4})$.

Cerite-(La), $[(\text{REE,Ca})_9(\text{Fe}^{3+},\text{Ca,Mg})(\text{SiO}_4)_3[\text{SiO}_3(\text{OH})]_4(\text{OH})_3]$, was found in agpaitic pegmatites at Mt. Yuksporr, Khibina Massif, Kola Peninsula, Russia (Pakhomovsky et al. 2002). Mt. Yuksporr is the only known locality where the lanthanum-dominant analog of cerite-(Ce) has been described so far.

Minerals related to cerite-(Ce) and cerite-(La) containing significant amounts of Al have been found at several localities, which include Kyschtym, Urals (Silberminz 1929), Niederbohrsch granite, Erzgebirge, Germany (Förster 2000), and the Afrikanda Complex, Kola Peninsula, Russia (Chakhmouradian and Zaitsev 2002). To date, no crystal-structure studies on such materials have been made. A study of Al-rich material from the Ratti quarry, Baveno, Verbania province, Piemonte region, Italy, has indicated this material to be the new species, aluminocerite-(Ce). Here it occurs in miarolitic cavities of NYF (niobium-yttrium-fluorine) granite pegmatites (Pezzotta et al. 1999).

The name aluminocerite-(Ce) reflects the fact that Ce is the

* E-mail: fabrizio.nestola@unipd.it

dominant REE, and that the octahedral *M* site is dominated by Al. The mineral was approved by the Commission on New Minerals, Nomenclature and Classification (CNMNC), IMA (IMA 2007-060). Holotype (inventory no. MM5200) and cotype (inventory no. MM5549) specimens are housed in the collection of the Museum of Mineralogy of the University of Padova, Italy. For this study, the holotype is designated as sample 1 and the cotype as sample 2. The holotype was approved by IMA before we could obtain data on the cotype. Because the quality of the collected single-crystal diffraction data of the cotype was much better, we have decided to report the crystal-structure refinement obtained on the cotype.

DESCRIPTION AND OCCURRENCE OF THE HOLOTYPE AND COTYPE OF ALUMINOCERITE-(Ce)

The holotype of aluminocerite-(Ce) was collected at the Ratti quarry in 2000 by A. Broggi and C. Tibiletti, two amateur mineralogists. This quarry is near Baveno, a renowned type-locality of several beryllium and scandium silicates, which include bavenite (Artini 1901), bazzite (Artini 1915), cascandite and jervisite (Mellini et al. 1982), and scandiobabingtonite (Orlandi et al. 1998), along with the REE-carbonate, calcioancylite-(Nd) (Orlandi et al. 1990). The holotype forms aggregates of up to 0.2 mm of pseudo-octahedral to rhombohedral crystals, flattened on the *c* axis (Fig. 1), that are pale pink to pink in color, with a vitreous luster. Single crystals are relatively small, from 5 to 10 μm exhibiting the dominant forms rhombohedron $\{10\bar{1}1\}$ and pinacoid $\{0001\}$ as observed in backscattered electron images (Fig. 2a). These are very similar to the forms reported by Pakhomovsky et al. (2002) in their Figure 1b. The minerals occur in millimeter-sized secondary cavities hosted in a laminated albite matrix, which forms aplite-pegmatite veins and pods in pink granite. These secondary cavities are formed by partial dissolution of gadolinite-group minerals (e.g., Pezzotta et al. 1999). The holotype of aluminocerite-(Ce) is associated with hingganite-(Y), Yb-rich hingganite-(Y), thorite, fluorite, albite, quartz, and K-feldspar (Fig. 2b).

The cotype of aluminocerite-(Ce) was collected at the Locately quarry, near Baveno, in 1968 by P. Tamea. Here the mineral develops in aggregates of pseudo-octahedral to rhombohedral crystals (up to 0.8 mm) that are pink-reddish in color. Single crystals have maximum dimensions of 50 μm (Fig. 3) and, as in the case of the holotype, the prevailing faces are the rhombohedron $\{10\bar{1}1\}$ and the pinacoid $\{0001\}$. The cotype occurs in centimeter-sized miarolitic cavities of pink granite and are associated with quartz, pinkish K-feldspar, white albite, green chamosite and whitish, prismatic submillimeter crystals of hingganite-(Y).

PHYSICAL AND OPTICAL PROPERTIES

Aluminocerite-(Ce) is translucent, pink to pink-reddish, and non-fluorescent. The streak is white and the luster is vitreous. The hardness based on the Mohs scale is 5 and the tenacity is brittle. No cleavage was observed and no fracture patterns were detected. The density could not be measured because of the small grain size. The calculated density is 4.675 g/cm^3 (from the empirical formula). Optically, no twinning was observed. Aluminocerite-(Ce) is uniaxial (+) with $\omega = 1.810\text{--}1.816$ and $\epsilon =$

1.812–1.822 ($\lambda = 589 \text{ nm}$). The dispersion could not be measured. The mineral is non-pleochroic. The calculated compatibility ($1 - K_p/K_c$) is superior (-0.014) (Mandarino 2007).

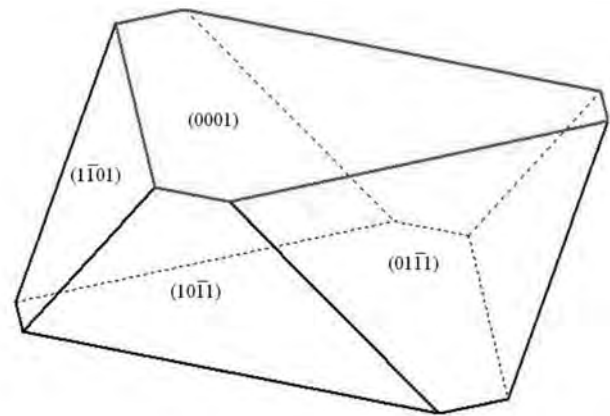


FIGURE 1. Representative sketch of the crystal forms observed in aluminocerite-(Ce).

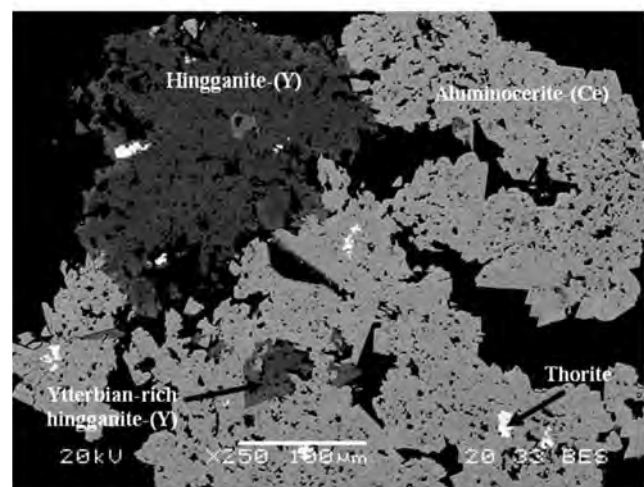
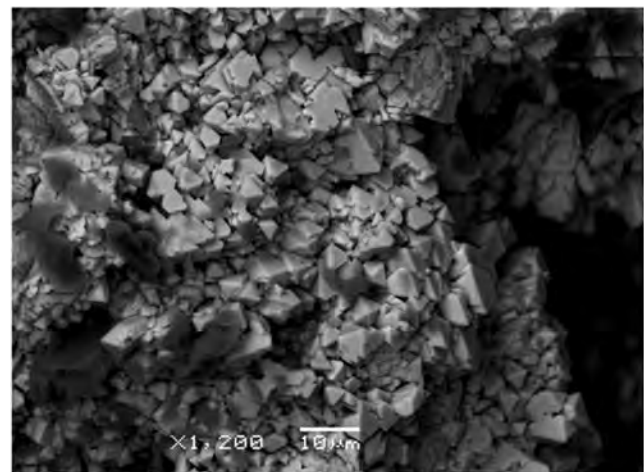


FIGURE 2. BSE images of the holotype of aluminocerite-(Ce) showing (a) pseudo-octahedral to rhombohedral crystals flattened on the *c* axis; (b) aluminocerite-(Ce) associated with hingganite-(Y), ytterbium-rich hingganite-(Y), thorite, fluorite, albite, quartz, and K-feldspar.

EXPERIMENTAL METHODS

Chemical analyses

Chemical analyses (15 points) were carried out using a Cameca SX-50 electron microprobe (WDS mode, 20 kV, 20 nA, 10 s counting times for peak and 5 s for background, 1–2 μm beam diameter). X-ray counts were converted to oxide wt% using the PAP correction program supplied by CAMECA (Pochou and Pichoir 1985). Natural minerals, synthetic phases, pure metals standards, spectral lines, and analytical crystals utilized were: wollastonite ($\text{SiK}\alpha$, TAP), wollastonite ($\text{CaK}\alpha$, PET), corundum ($\text{AlK}\alpha$, TAP), fluorapatite ($\text{PK}\alpha$, $\text{FK}\alpha$, TAP), synthetic periclase ($\text{MgK}\alpha$, TAP), hematite ($\text{FeK}\alpha$, LiF), synthetic MnTiO_3 ($\text{FeK}\alpha$, LiF), synthetic Y-RE-phosphates ($\text{YL}\alpha$, PET; $\text{REL}\alpha$ and $\text{NdL}\beta$, $\text{GdL}\beta$, $\text{DyL}\beta$ LiF). The H_2O content could not be determined directly due to a paucity of material and was therefore determined by stoichiometry. However, the presence of water was confirmed by microRaman spectroscopy, described in the following section. All the iron was considered as Fe^{3+} from consideration of average bond lengths and cation radii.

Raman spectroscopy

Raman spectra for sample 1 were collected with a home-built micro-Raman system, based on a single 320 mm focal length imaging spectrograph, a Triax-320 ISA instrument, equipped with a holographic 1800 g/mm grating and a liquid-nitrogen-cooled CCD detector (Spectrum One ISA Instruments). The excitation source was a Spectra Physics Ar⁺ laser (Stabilite 2017-06S) operating at 514.5 nm. A Kaiser Optical System holographic notch filter (514.5 nm) was used to reduce the stray-light level. An Olympus BX 40 optical microscope equipped with three objectives, 20 \times /0.35, 50 \times /0.75, and 100 \times /0.90 was optically coupled to the spectrograph.

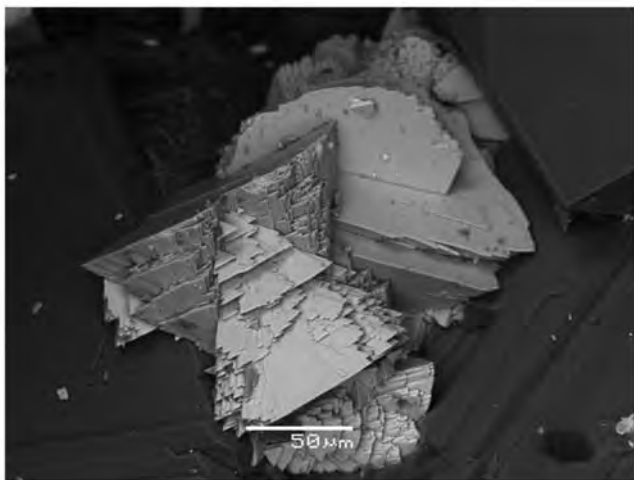


FIGURE 3. BSE images of the cotype of aluminocerite-(Ce).

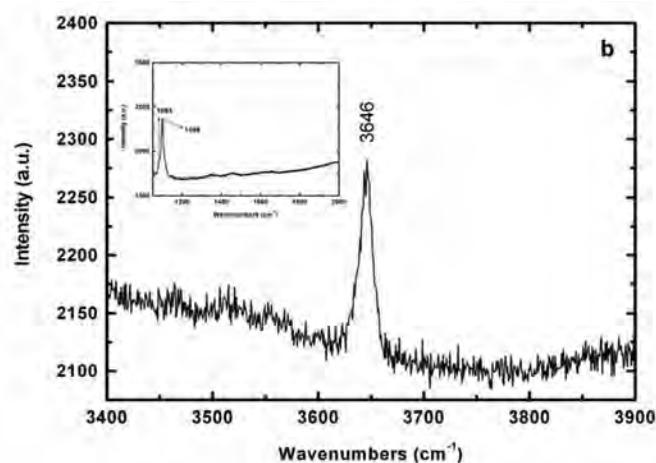
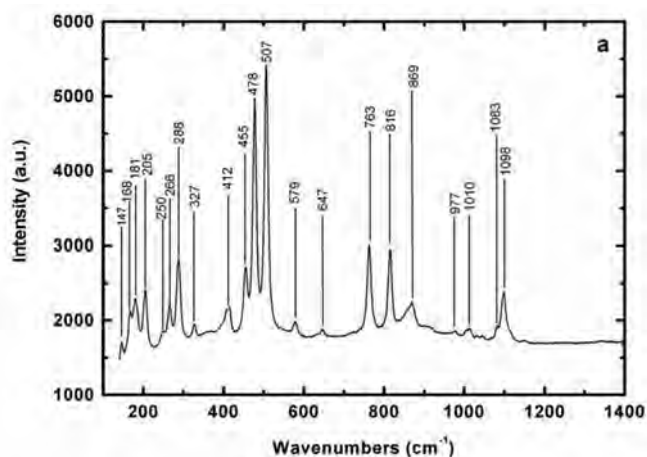


FIGURE 4. Raman spectra for aluminocerite-(Ce). (a) Low-frequency region showing mainly vibrational modes of cation-oxygen interactions. (b) Detail of high-frequency region showing the stretch vibration mode of (OH) groups (in the insert the region of the spectrum between 1000 and 2000 cm^{-1} is shown).

This made it possible to observe the sample with the microscope and to then select particular micrometric regions for Raman analysis. With the 100 \times objective, the lateral resolution is estimated to be 0.5 μm and the depth of focus between 1–2 μm . To avoid optical damage to the sample, the power of the exciting radiation was maintained between 10 and 50 mW. The Raman spectra were recorded between 147 and 3900 cm^{-1} with an instrumental resolution of about 2 cm^{-1} . The resulting Raman spectrum of aluminocerite-(Ce) is reported in Figures 4a and 4b.

No precise assignment was made for the observed vibrational modes. Still, useful information can be extracted. In the recorded Raman spectra, there are no indications for the presence of light elements like BO_3 groups (no bands in the 1400–1300 cm^{-1} region). The 1100 cm^{-1} band can be attributed to the SiO_4 stretching vibration, and the strong bands in the 500 cm^{-1} region to bending modes of SiO_4 groups. Bands in the energy region below 400 cm^{-1} are usually caused by vibrations of the larger cations with high coordination number (e.g., REE elements and Ca in the structure). The Raman spectra also helped to gain insight into H speciation (as we will discuss in the corresponding section).

Single-crystal X-ray diffraction

A single crystal was extracted from the holotype (sample 1) and cotype (sample 2) and investigated by X-ray diffraction. As described above, the mineral occurs in aggregates of small crystals (Figs. 1a and 2) making separation of a single crystal very difficult. The size of the crystals eventually suitable for single-crystal diffraction was markedly small for both of the samples. Both crystals were checked optically and found to produce a relatively sharp extinction. Intensity data were collected using a STOE single-crystal diffractometer equipped with an Oxford Diffraction CCD detector over a range of $5 \leq 2\theta \leq 70^\circ$ using a 0.2° ω -scan with exposure time of 60 s. The sample-detector distance was 60 mm. The program CrysAlis RED (Oxford Diffraction) was used to integrate the intensity data, applying the Lorentz-polarization correction, while the X-RED (Stoe and Cie 2001) and X-SHAPE (Stoe and Cie 1999) programs were used to correct for absorption. Lattice parameters were obtained by refining the positions of 1226 reflections. The observed c/a ratios were 3.585 (sample 1) and 3.571 (sample 2).

Weighted structural refinements were done in space group $R3c$ using the SHELX-97 package (Sheldrick 1997), starting from the atomic coordinates of Moore and Shen (1983). Atomic scattering curves were taken from the *International Tables for X-ray Crystallography* (Ibers and Hamilton 1974). Unfortunately, the small size and poor diffraction quality of sample 1 resulted in an unstable refinement. An increase in the exposure time (to max 75 s) of the data collection did not provide significantly better results. Conversely, for sample 2, despite its small size, we could obtain a structure refinement with an agreement factor lower than 6%, and it is this structure that is described herein. Site occupancies were refined for the REE(1,2,3) sites using the scattering curve of Ce. For the M site, we used both Al and Fe^{3+} scattering curves and assumed full occupancy. The occupancies of the Si sites and O sites were fixed. With the model at convergence, the site occupancy factors of Si3 and OH10 were permitted to vary to check if these sites were fully occupied, as they have been reported as partially occupied in cerite-(La) by Pakhomovsky et al. (2002). The refinement did not show any significant deviation

from full occupancy and they were subsequently fixed in the last cycles. Anisotropic displacement parameters were refined for all the crystallographic sites. Unit-cell parameters of both crystals from samples 1 and 2, and crystal structure refinement details for the crystal from sample 2 are reported in Table 1, along with the reported data for cerite-(Ce) (Moore and Shen 1983) and cerite-(La) (Pakhomovsky et al. 2002) for comparison purposes. The atomic coordinates, site occupancy factors, and displacement parameters are reported in Table 2. Selected bond lengths are reported in Table 3. A complete list of observed and calculated structure factors and the CIF file have been deposited.¹

Calculated X-ray powder pattern

Due to the few crystals available and to the differences in composition, the X-ray powder-diffraction pattern for CuK α , requested for the description of a new mineral, was calculated from the single-crystal data and is reported in Table 4.

¹ Deposit item AM-09-018, the CIF file and the list of observed and calculated structure factors. Deposit items are available two ways: For a paper copy contact the Business Office of the Mineralogical Society of America (see inside front cover of recent issue) for price information. For an electronic copy visit the MSA web site at <http://www.minsocam.org>, go to the American Mineralogist Contents, find the table of contents for the specific volume/issue wanted, and then click on the deposit link there.

RESULTS AND DISCUSSION

The octahedral *M* site and tetrahedral Si sites

The octahedral *M* site of aluminocerite-(Ce) is dominated by Al with only minor Fe, as inferred from EMPA data (Table 5). As the cation radius of Al in octahedral coordination is 0.535 Å (Shannon 1976) and the observed mean bond length at the *M* site is 1.931 Å (Table 3), it suggests that iron has to be in the trivalent state ($r = 0.645$ Å). The chemical composition obtained for the *M* site in sample 2 (Al_{0.70}Fe_{0.25}³⁺) corresponding to 15.6 electrons per formula unit (epfu) should be compared to 18.1(5) epfu obtained from the structure refinement (Table 2). The agreement is reasonable and probably indicates a slightly lower Al concentration in the studied crystal. A site occupancy of (Al_{0.61}Fe_{0.39}³⁺) corresponds to a calculated mean bond distance of 1.956 Å, close to the refined value and within the observed errors for individual distances. If the Fe present were only Fe²⁺ in octahedral coordination we would expect a mean bond length of 1.997 Å, significantly greater than the observed value of 1.931 Å. Consistent with our choice, Holtstam and Andersson (2007)

TABLE 1. Crystal structure refinement details for aluminocerite-(Ce) (sample 2) and comparison of unit-cell parameters with aluminocerite-(Ce) (sample 1) and reported data for cerite-(La) (Pakhomovsky et al. 2002) and cerite-(Ce) (Moore and Shen 1983)

	Aluminocerite-(Ce) (sample 2)	Aluminocerite-(Ce) (sample 1)	Cerite-(La)*	Cerite-(Ce) †
<i>a</i> (Å)	10.645(1)	10.581(4)	10.7493(6)	10.779(6)
<i>c</i> (Å)	38.019(5)	37.932(9)	38.318(3)	38.061(7)
<i>V</i> (Å ³)	3731.0	3677.8	3834.4	3829.8
space group	<i>R</i> 3c	<i>R</i> 3c	<i>R</i> 3c	<i>R</i> 3c
<i>Z</i>	6	6	6	6
crystal size (mm)	0.040 × 0.030 × 0.025	0.025 × 0.010 × 0.015	0.280 × 0.280 × 0.120	0.09 × 0.11 × 0.12
radiation	MoK α	MoK α	MoK α	MoK α
total reflections	3282		7189	7262
unique reflections	1795		1983	1711
2 θ_{\max} (°)	70			65
Unique $F_o \geq 4\sigma$	754		1544	
<i>R</i> 1	0.056		0.036	0.032
<i>wR</i> ²	0.140		0.079	
Goodness of Fit (<i>S</i>)	0.81		0.926	
refinement method	SHELXL-97		SHELXTL	SHELX-76

* Pakhomovsky et al. (2002).

† Moore and Shen (1983).

TABLE 2. Atomic coordinates ($\times 10^4$) and equivalent isotropic displacement parameters ($\text{Å}^2 \times 10^3$) for aluminocerite-(Ce) (sample 2)

Atom	s.o.f.	<i>x</i>	<i>y</i>	<i>z</i>	<i>U</i> _{eq}	<i>U</i> ₁₁	<i>U</i> ₂₂	<i>U</i> ₃₃	<i>U</i> ₂₃	<i>U</i> ₁₃	<i>U</i> ₁₂
REE1	Ce = 0.92(1)	0.25920(17)	0.13369(18)	0.06808(5)	0.0233(4)	0.0239(8)	0.0234(8)	0.0232(7)	-0.0008(7)	0.0001(6)	0.0122(7)
REE2	Ce = 0.82(1)	0.14123(18)	0.2582(2)	0.43098(7)	0.0224(4)	0.0212(9)	0.0248(9)	0.0227(8)	0.0049(7)	0.0022(10)	0.0125(8)
REE3	Ce = 0.616(8)	0.2572(2)	0.1337(2)	0.1759	0.0230(5)	0.0242(10)	0.0215(11)	0.0252(9)	-0.0039(9)	-0.0043(8)	0.0128(9)
Si1		0.3167(8)	0.1467(8)	0.36201(18)	0.0234(16)	0.024(3)	0.023(4)	0.021(4)	0.000(3)	-0.002(3)	0.010(3)
Si2		0.1499(8)	0.3268(9)	0.1372(2)	0.0231(14)	0.026(4)	0.018(3)	0.024(3)	0.007(2)	0.003(3)	0.010(3)
Si3		0	0	0.2531(4)	0.027(2)	0.022(2)	0.022(2)	0.036(6)	0.000	0.000	0.0109(12)
M1	Al = 0.61(4) Fe ³⁺ = 0.39(4)	0	0	-0.0014(3)	0.026(2)	0.027(2)	0.027(2)	0.024(4)	0.000	0.000	0.0136(12)
O1*		0.256(2)	0.090(2)	-0.0014(3)	0.026(2)	0.027(2)	0.027(2)	0.024(4)	0.000	0.000	0.0136(12)
O2		0.277(2)	0.0044(16)	0.3228(5)	0.035(5)	0.028(9)	0.046(12)	0.022(8)	-0.002(8)	-0.005(7)	0.012(9)
O3		0.265(3)	0.250(2)	0.3854(5)	0.025(4)	0.032(9)	0.012(7)	0.033(9)	-0.008(6)	0.001(8)	0.011(7)
O4		0.083(2)	0.1684(18)	0.3782(5)	0.034(5)	0.036(11)	0.030(11)	0.039(13)	0.003(9)	0.005(9)	0.019(10)
O5		0.244(2)	0.268(2)	0.0297(4)	0.029(4)	0.051(13)	0.012(7)	0.024(8)	0.005(6)	0.006(10)	0.015(9)
O6		-0.018(2)	0.269(2)	0.1158(5)	0.037(5)	0.030(11)	0.028(10)	0.046(13)	0.002(9)	0.009(9)	0.010(9)
O7		0.1637(18)	0.0719(19)	0.1227(6)	0.035(5)	0.037(11)	0.036(11)	0.038(11)	-0.001(9)	-0.005(9)	0.024(9)
O8		0.142(2)	0.2790(15)	0.4679(5)	0.027(4)	0.014(7)	0.013(7)	0.053(12)	0.007(8)	0.006(7)	0.006(7)
O9		0.1626(14)	0.038(2)	0.1783(5)	0.024(3)	0.017(8)	0.016(6)	0.033(8)	-0.003(6)	0.001(7)	0.004(7)
OH10		0	0	0.2404(5)	0.050(6)	0.046(12)	0.044(13)	0.043(12)	-0.011(9)	-0.017(10)	0.010(10)
OH11		0	0	0.2972(5)	0.024(6)	0.012(6)	0.012(6)	0.047(19)	0.000	0.000	0.006(3)
OH12		0	0	0.0921(11)	0.029(7)	0.004(6)	0.004(6)	0.08(2)	0.000	0.000	0.002(3)
OH13		0	0	0.1607(7)	0.018(4)	0.011(6)	0.011(6)	0.033(12)	0.000	0.000	0.006(3)

* O1 is probably a hydroxyl.

TABLE 3. Selected bond lengths (Å) for aluminocerite-(Ce) (sample 2)

REE1-O5	2.36(2)	REE3-O8	2.41(2)
REE1-O8a	2.45(2)	REE3-OH(12)	2.441(6)
REE1-O6b	2.51(2)	REE3-O6b	2.47(2)
REE1-O4	2.55(2)	REE3-O2e	2.52(2)
REE1-OH11	2.56(1)	REE3-O3a	2.52(2)
REE1-O4b	2.57(2)	REE3-O8b	2.55(2)
REE1-O2c	2.60(2)	REE3-O9	2.66(2)
REE1-O3d	2.74(2)	REE3-O5	2.73(2)
REE1-O9e	2.81(2)	REE3-O1e	2.97(2)
<REE1-O>	2.573	<REE3-O ₉ >	2.585
		<REE3-O ₈ >*	2.537
REE2-O2f	2.38(2)		
REE2-O3	2.43(2)	Si1-O3	1.58(2)
REE2-O9g	2.46(2)	Si1-O1	1.62(2)
REE2-O7f	2.50(2)	Si1-O2	1.62(2)
REE2-OH13	2.52(1)	Si1-O4h	1.68(2)
REE2-O7	2.54(2)	<Si1-O>	1.624
REE2-O5h	2.61(2)		
REE2-O1g	2.65(2)	Si(2)-O7d	1.63(2)
REE2-O6i	2.80(2)	Si(2)-O8	1.63(2)
<REE2-O>	2.542	Si2-O5	1.64(2)
		Si2-O6	1.67(2)
		<Si2-O>	1.642
M-O7j,k,l ×3	1.91(2)	Si3-OH10	1.68(2)
M-O4,b,e	1.95(2)	Si3-O9,b,f ×3	1.64(1)
<M-O>	1.931	<Si3-O>	1.649

Notes: Symmetry transformations used to generate equivalent atoms: a = -y + 2/3, -x + 1/3, z - 1/6; b = -x + y, -x, z; c = -y + 1/3, x - y - 1/3, z - 1/3; d = -x + y + 1/3, -x + 2/3, z - 1/3; e = -x + y + 2/3, y + 1/3, z - 1/6; f = -y, x - y, z; g = -y + 1/3, -x + 2/3, z + 1/6; h = -y + 2/3, x - y + 1/3, z + 1/3; i = -x + y - 1/3, -x + 1/3, z + 1/3; j = -y, -x, z + 1/2; k = -x + y, y, z + 1/2; l = x, x - y, z + 1/2.

* Mean bond distance calculated considering eightfold coordination for this site.

TABLE 4. X-ray powder-diffraction data for aluminocerite-(Ce) (CuKa)

hkl	Aluminocerite-(Ce)			Cerite-(Ce)		Cerite-(La)	
	<i>d_{hkl}</i> (meas)	<i>d_{hkl}</i> (calc)	Intensity (%)	<i>d_{hkl}</i> (meas)	Intensity (%)	<i>d_{hkl}</i> (meas)	Intensity (%)
202	4.454	4.454	16	4.53	17	4.53	20
122	3.405	3.407	27	3.47	42	3.47	40
124	3.250	3.253	26	3.31	33	3.31	38
030	3.053	3.054	19	3.11	30	3.10	25
02,10	2.914	2.922	100	2.95	100	2.958	100
218	2.800	2.797	23	2.83	38	2.833	37
220	2.647	2.645	58	2.69	42	2.689	34
01,16	2.293	2.295	16			2.315	12
03,12	2.198	2.197	40	2.22	25	2.223	22
238	1.923	1.922	34	1.954	50	1.949	34
051	1.826	1.824	24			1.863	14
054	1.798	1.799	20	1.834	12	1.828	12
330	1.762	1.763	8	1.799	15	1.792	12
03,18	1.732	1.735	46	1.748	25	1.755	23
428	1.625	1.627	4	1.655	7	1.652	6
23,16	1.572	1.573	11	1.593	13	1.593	12

Notes: The "measured" powder data for aluminocerite were obtained from calculation on the basis of the single-crystal X-ray diffraction data from this work. The data for cerite-(Ce) come from Glass et al. (1958), and those of cerite-(La) from Pakhomovsky et al. (2002).

report that, on the basis of Mössbauer spectrometry obtained on two samples of cerite-(Ce), about 80% Fe is in the trivalent state, with chemical shifts of 0.33–0.35 corresponding to Fe³⁺ ions in octahedral coordination. The reported mean bond lengths for the *M* site are 2.072 Å cerite-(Ce) (Moore and Shen 1983) and 1.99 Å cerite-(La) (Pakhomovsky et al. 2002). While a calculated value of 2.09 Å is reported for cerite-(Ce) by Moore and Shen (1983) considering a composition for the *M* site of (Mg_{0.61}Fe_{0.39}), the reported composition in Table 4 of Moore and Shen (1983) (Mg_{0.86}Al_{0.41}Fe_{0.21}Mn_{0.05}Ti_{0.02})_{Σ=1.55} does not agree with such assigned site population. The reported formula (Fe_{0.32}Ca_{0.30}Mg_{0.23})_{Σ=0.85} for

TABLE 5. Chemical compositions of aluminocerite-(Ce) samples

Oxides (wt%)	Sample 1	σ	Sample 2	σ
Ce ₂ O ₃	23.37	2.8	29.68	2.5
Nd ₂ O ₃	15.59	1.5	10.93	1.8
La ₂ O ₃	7.43	1.1	12.52	1.2
Sm ₂ O ₃	4.38	0.9	1.55	0.44
Pr ₂ O ₃	3.54	0.7	4.01	0.8
Gd ₂ O ₃	3.12	0.6	0.94	0.2
Y ₂ O ₃	1.68	0.4	1.66	0.3
Dy ₂ O ₃	0.46	0.1	0.29	0.1
Yb ₂ O ₃	0.07	0.02	0.11	0.03
CaO	8.31	0.9	7.28	0.7
Fe ₂ O ₃ *	0.47	0.08	1.11	0.11
MnO	b.d.l.		b.d.l.	
MgO	b.d.l.		b.d.l.	
Al ₂ O ₃	2.47	0.6	2.01	0.5
SiO ₂	24.01	1.1	23.76	1.2
P ₂ O ₅	b.d.l.		b.d.l.	
F	b.d.l.		b.d.l.	
H ₂ O †	3.63		3.30	
Total	98.53		99.37	

Notes: b.d.l. indicates below detection limit; σ is the standard deviation and indicates the chemical variability of the analyzed sample.

* All Fe as Fe³⁺.

† H₂O obtained by stoichiometry.

cerite-(La) implies 0.15 vacancies pfu. Moreover, Pakhomovsky et al. (2002) report up to 0.30 pfu of Ca at the *M* site. Considering the reduced dimension of this site, it is highly improbable that Ca enters it (the ionic radius of Ca in sixfold coordination is 1.00 Å, implying a mean bond length of 2.38 Å for a site completely occupied by this element). Up to 1 wt% of Al₂O₃ is present in that sample (Sergey Krivovichev, personal communication), which corresponds to 0.36 apfu of Al. With a composition of (Al_{0.36}Fe_{0.32}Mg_{0.23})_{Σ=0.91} for the *M* site, the calculated mean bond length is 1.98 Å, in fairly good agreement with the mean bond length reported by Pakhomovsky et al. (2002). Interestingly, the bond valence calculations reported by Pakhomovsky et al. (2002) yield a bond valence sum of 3.22 valence units (v.u.) at the *M* site, in good agreement with the dominant charge at the *M* site being 3. Hence it is very likely that cerite-(La) is actually an aluminocerite-(La).

Silicon is present in isolated SiO₄ groups in the cerite structure. The three tetrahedral sites (Si1, Si2, and Si3) present in the structure of aluminocerite-(Ce) have been considered all fully occupied, based on the results for cerite-(Ce) and cerite-(La). The mean bond length <Si1-O> = 1.62 Å is, within error, the same as that in cerite-(Ce) (1.63 Å) and cerite-(La) (1.64 Å), while the mean bond length <Si2-O> = 1.642 Å is also comparable to those in both cerite-(Ce) and cerite-(La) (1.62 and 1.63 Å, respectively).

The Si3 site is the largest tetrahedral site in the structure and shows three equal bond lengths (Si3-O9 = 1.64 Å) and one markedly longer bond length Si3-O10 = 1.67 Å, typical of the presence of (OH) in a silanol group. The average <Si3-O> bond length is 1.65 Å for aluminocerite-(Ce), consistent with those for cerite-(Ce) (1.64 Å), and cerite-(La) (1.65 Å).

REE polyhedra

Three REE polyhedra are present in the cerite crystal structure: REE1, REE2, and REE3. We follow the naming of the sites chosen in previous work. Refinement of the site occupation factor (s.o.f.) of REE3 site gave a significantly lower refined

site scattering compared to the previous published cerite refinements: in aluminocerite-(Ce), the s.o.f. is 0.62, corresponding to a scattering power of 36 electrons per site (eps); in cerite-(Ce), the reported s.o.f. is 0.879(5), or 50.98 eps; in cerite-(La), the reported s.o.f. for La is 0.741(6), or 42.24 eps. We also observe that the Ca content is higher in aluminocerite compared to the values reported for cerite-(Ce) and cerite-(La): 2.60 pfu in sample 1 and 2.30 pfu in sample 2, in aluminocerite-(Ce) (Table 5); 1.63 pfu in cerite-(Ce) and 1.67 pfu in cerite-(La). The average bond lengths in the three REE-O₈ polyhedra, described in cerite-(Ce) (Moore and Shen 1983) are <REE1-O> = 2.595 Å, <REE2-O> = 2.546 Å, and <REE3-O> = 2.610 Å. In cerite-(La), Pakhomovsky et al. (2002) report three REE-O₉ polyhedra with mean bond lengths of <REE1-O> = 2.59 Å, <REE2-O> = 2.56 Å, and <REE3-O> = 2.61 Å. Aluminocerite-(Ce) has REE1 and REE2 in ninefold coordination with average bond lengths of 2.573 and 2.542 Å, respectively. In the REE3 site, assuming ninefold coordination, the observed longest distance (REE3-O1) is 2.970 Å, which appears to be likely too long for a site more than half-occupied by Ca, and it is possible that the actual coordination for REE3 polyhedron is 8 in aluminocerite-(Ce). Taking into account the chemical analyses and the refined s.o.f. in the structure refinement, we propose the following cation distribution for the REE sites and show the relative agreement of observed s.o.f. (s.o.f._{obs}) and calculated s.o.f. (s.o.f._{calc}) in electrons per site (eps):

REE1 = (Nd_{0.38}Ce_{0.34}Pr_{0.14}Sm_{0.05}Gd_{0.02}Dy_{0.01}Yb_{0.003}) [s.o.f._{obs} 53.4(5), s.o.f._{calc} 56.7]

REE2 = (Ce_{0.55}La_{0.24}Ca_{0.20}) [s.o.f._{obs} 47.6(5), s.o.f._{calc} 49.6]

REE3 = (Ca_{0.57}La_{0.21}Ce_{0.18}) [s.o.f._{obs} 35.7(5), s.o.f._{calc} 33.8]

with an overall agreement within 3% relative error.

The distribution of REE for aluminocerite-(Ce) is also significantly different from that in cerite-(La): if we consider the three most abundant REE for our samples we observe a strong decrease in La and a significant increase in Nd with respect to the cerite-(La), whereas the Ce content of cerite-(La) is intermediate between that of sample 1 and sample 2:

Aluminocerite-(Ce), sample 1: Ce_{2.49}Nd_{1.62}La_{0.80}

Aluminocerite-(Ce), sample 2: Ce_{3.20}Nd_{1.15}La_{1.36}

Cerite-(La) (Pakhomovsky et al. 2002): Ce_{2.65}Nd_{0.16}La_{4.23}

The observed differences are probably related to the geochemical environment in which the different cerite specimens grew, with a strong fractionation of light-REE in the sample from Khibina Massif in the Kola Peninsula, corresponding to the alkaline rocks in which cerite-(La) is part of a late secondary assemblage. The analysis of cerite-(Ce) provided by Moore and Shen (1983), who reported the analyses of Glass et al. (1958), disclose only the Ce concentration and the rest of the REE are aggregated to La. We cannot therefore compare these values with the composition of our material.

Hydrogen speciation in aluminocerite-(Ce)

Owing to the small amount of material available, the amount of water could not be determined (e.g., common experimental techniques like polarized FTIR spectroscopy could not be used,

and, moreover, no standards are available). However, Raman micro-spectroscopy (Fig. 4b) gave a definitive proof that (OH) is present (the band at about 3650 cm⁻¹), and no H₂O molecules were detected; the typical H₂O bending band at about 1600 cm⁻¹ is not present in the spectrum (Fig. 4b).

Previous works on cerite-(Ce) and cerite-(La) left open some debate concerning the hydrous content of cerite. Pakhomovsky et al. (2002) obtained a bond valence sum of 1.36 v.u. at the O1 site, a typical value for an (OH) group. Performing the same calculation for O1 using the atom coordinates of Moore and Shen (1983) in cerite-(Ce), a value of 1.19 v.u. is obtained. Therefore, Pakhomovsky et al. (2002) proposed for both cerite-(Ce) and cerite-(La) the presence of four SiO₃(OH) and three SiO₄ groups pfu, whereas Moore and Shen (1983) proposed one SiO₃(OH) and six SiO₄ groups. Bond-valence calculations performed using our atom coordinates for aluminocerite-(Ce) (using bond-valence parameters for Ce³⁺-O and Si⁴⁺-O bonds; Brown 1993) give a value of 1.44 v.u. for O1, very close to that determined by Pakhomovsky et al. (2002) for cerite-(La). Thus we consider that O1 is occupied by an (OH) group. This is also in agreement with the observation of a longer REE3-O1 distance (see above). Therefore, our chemical formula for aluminocerite-(Ce) is also based on four SiO₃(OH) and three SiO₄ groups pfu.

Proposed crystal formulae and ideal formula of aluminocerite-(Ce)

The chemical formulae were calculated from the chemical analyses reported in Table 5 on the basis of 7 Si atoms, and considering the presence of (OH) groups (see previous section). The formulae for the two samples are:

Sample 1—

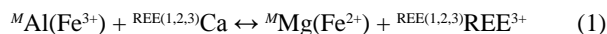
(Ca_{2.60}Ce_{2.49}Nd_{1.62}La_{0.80}Sm_{0.44}Pr_{0.38}Gd_{0.30}Y_{0.26}Dy_{0.04}Yb_{0.01})_{Σ8.94}(Al³⁺_{0.85}Fe³⁺_{0.10})_{Σ0.95}(SiO₄)₃[SiO₃(OH)]₄(OH)_{3.06}

Sample 2—

(Ce_{3.20}Ca_{2.30}La_{1.36}Nd_{1.15}Pr_{0.43}Y_{0.26}Sm_{0.16}Gd_{0.09}Dy_{0.03}Yb_{0.01})_{Σ8.99}(Al³⁺_{0.70}Fe³⁺_{0.25})_{Σ0.95}(SiO₄)₃[SiO₃(OH)]₄(OH)_{2.48}O_{0.52}.

The ideal formula is (Ce₆Ca₃)_{Σ9}(Al)(SiO₄)₃[SiO₃(OH)]₄(OH)₃, which would require the following: Ce₂O₃ 58.36, CaO 9.97, Al₂O₃ 3.02, SiO₂ 24.92, H₂O 3.73, Total 100 wt%.

The substitution of divalent cations at the M site can be charge balanced by the following reaction:



which has also been previously proposed by Holtstam and Andersson (2007), although these authors did not have support from direct structural evidence.

Moore and Shen (1983) described a site with partial occupancy that they named Ca(x). In cerite-(Ce), this has 0.169(9) Ca apfu (Moore and Shen 1983; Table 5), while the same site has been described by Pakhomovsky et al. (2002) in cerite-(La) with partial occupancy of 0.10 apfu. The structure of aluminocerite-(Ce) does not possess this Ca site. As discussed by Pakhomovsky et al. (2002), the presence of this site implies Si deficiency as Ca and Si3 cannot be present simultaneously [the Ca-Si3 distance

in cerite-(La) is 2.19 Å]. Therefore, partial occupation of the Ca site also implies the loss of an O atom and possibly the H attached to the OH(10) anion. However, only SiO is required to balance the entrance of Ca:



and the H forming part of the OH10 anion can bond locally to another underbonded anion, like OH13, which shows the longest bond lengths with La2 and a lower calculated bond valence sum.

The effect of the dominance of a small cation on the *M* site is important, as a difference of up to 4% in lattice volume is observed between cerite-(Ce) and aluminocerite-(Ce) (Table 1), while only a 0.12% difference is observed between cerite-(Ce) and cerite-(La). The chemical compression effect occurs mainly in the (0001) plane. The SiO₄ groups adapt as rigid bodies to the collapse of the *M* site while the REE(1,2,3) sites adapt to the deformation. Therefore, a smaller cell volume may be a good indication of Al being the dominant species on the *M* site and of small cations on the REE(1,2,3) sites.

ACKNOWLEDGMENTS

The authors want to thank S. Krivovichev, R. Thompson, A. McDonald, and I.P. Swainson for their careful and extremely helpful review that strongly improved the manuscript. Financial support has been provided by MIUR PRIN 2006047943 to A. Dal Negro. Fernando Cámara was supported by funding by CNR-IGG through the project TAP01.004.002. R. Carampin of CNR-Padova for WDS electron microprobe facilities.

REFERENCES CITED

- Artini, E. (1901) Di una nuova specie trovata nel granito di Baveno. *Atti della Reale Accademia dei Lincei. Rendiconti. Classe di scienze fisiche, matematiche e naturali*, 10, 139–145.
- (1915) Due minerali di Baveno contenenti terre rare: weibeite e bazzite. *Atti della Reale Accademia dei Lincei. Rendiconti. Classe di scienze fisiche, matematiche e naturali*, 24, 313–319.
- Brown, I.D. (1993) Bond valence calculator (software). Institute for Materials Research, McMaster University, Hamilton, Ontario, Canada.
- Chakhmouradian, A.R. and Zaitsev, A.N. (2002) Calcite-amphibole-clinopyroxene from the Afrikanda Complex, Kola Peninsula, Russia: Mineralogy and a possible link to carbonatites. III. Silicate minerals. *Canadian Mineralogist*, 40, 1347–1374.
- Förster, H.J. (2000) Cerite-(Ce) and thorian synchysite-(Ce) from the Niederbobritzsch granite, Erzgebirge, Germany: Implications for the differential mobility of the LREE and Th during alteration. *Canadian Mineralogist*, 38, 67–79.
- Gay, P. (1957) The crystallography of cerite. *American Mineralogist*, 42, 429–432.
- Glass, J.J., Evans, H.T., Carron, M.K., and Rose, H. (1958) Cerite from Mountain Pass, San Bernardino County, California. *American Mineralogist*, 41, 665–666.
- Hisinger, W. and Berzelius, J.J. (1804) Cerium, en ny Metall, funnen i Bastnäs Tungsten från Riddarhyttan i Westmanland. Henrik A. Nordström, Stockholm, Sweden.
- Holtstam, D. and Andersson, U.B. (2007) The REE minerals of the Bastnäs-type deposits, South-Central Sweden. *Canadian Mineralogist*, 45, 1073–1114.
- Ibers, J.A. and Hamilton, W.C. (1974) *International Tables for X-ray Crystallography*, IV. Kynoch Press, Birmingham, U.K.
- Mandarino, J.A. (2007) The Gladstone-Dale compatibility of minerals and its use in selecting mineral species for further study. *Canadian Mineralogist*, 45, 1307–1324.
- Mellini, M., Merlino, S., Orlandi, P., and Rinaldi, R. (1982) Cascandite and jervisite, two new scandium silicates from Baveno, Italy. *American Mineralogist*, 67, 599–603.
- Moore, P.B. and Shen, J. (1983) Cerite, RE₉(Fe³⁺,Mg)(SiO₄)₆(SiO₃OH)(OH)₃: its crystal structure and relation to whitlockite. *American Mineralogist*, 68, 996–1003.
- Orlandi, P., Pasero, M., and Vezzalini, G. (1990) Calcio-ancylite-(Nd), a new REE-carbonate from Baveno, Italy. *European Journal of Mineralogy*, 2, 413–418.
- (1998) Scandiobabingtonite, a new mineral from the Baveno pegmatite, Piedmont, Italy. *American Mineralogist*, 83, 1330–1334.
- Pakhomovsky, Y.A., Men'shikov, Y.P., Yakovenchuk, V.N., Ivaniuk, G.Y., Krivovichev, S.V., and Burns, P.C. (2002) Cerite-(La), (La,Ce,Ca)₉(Fe,Ca,Mg)(SiO₄)₆[SiO₃(OH)]₆(OH)₃, a new mineral species from the khibina alkaline massif: Occurrence and crystal structure. *Canadian Mineralogist*, 40, 1177–1184.
- Pezzotta, F., Diella, V., and Guastoni, A. (1999) Chemical and paragenetic data on gadolinite-group minerals from Baveno and Cuasso al Monte, Southern Alps, Italy. *American Mineralogist*, 84, 782–789.
- Pouchou, J.L. and Pichoir, F. (1985) "PAP" (phi-rho-z) procedure for improved quantitative microanalysis. In J.T. Armstrong, Ed., *Microbeam Analysis*. San Francisco Press, California.
- Shannon, R.D. (1976) Revised effective ionic radii and systematic studies of interatomic distances in halides and chalcogenides. *Acta Crystallographica*, A32, 751–767.
- Sheldrick, G.M. (1997) SHELX, Programs for crystal structure analysis. University of Göttingen, Germany.
- Silberminz, V. (1929) Sur le gisement de cerite de bastnaesite et d'un mineral nouveau, la lessingite dans le district de kychtym (Oural) Abs. *Neues Jahrbuch für Mineralogie, Kristallographie und Petrographie*, 1, 123–124.
- Stoe and Cie (1999) *Crystal Optimization for Numerical Absorption Correction*. Stoe and Cie GmbH, Darmstadt, Germany.
- (2001) *Data Reduction Program*. Stoe and Cie GmbH, Darmstadt, Germany.

MANUSCRIPT RECEIVED JULY 26, 2008

MANUSCRIPT ACCEPTED DECEMBER 2, 2008

MANUSCRIPT HANDLED BY IAN SWAINSON